Journal of Computer Engineering
ISSN 10003428

Original Research Article
Vol 12, Issue 6, 2023 | ISSN: 1000-3428

Analyzing Fan-Airframe Aerodynamic Interactions using a Machine Learning-Based Body Force Model

Maya Singh and Ethan Kim

Maya Singh, Department of Aerospace Engineering, Purdue University;

ABSTRACT

Body force modeling is a numerical strategy that allows an accurate representation of the aerodynamics of turbomachinery blade rows at a reduced computational cost, making it suitable for predicting fan-airframe aerodynamic interactions in boundary layer ingestion (BLI) propulsive architectures. This paper focuses on a new approach for building the body force representation using a machine learning technique, rather than analytically modeling the effects of the blades in the flow. This methodology is developed and assessed in a distorted inflow case representative of a BLI configuration and compared to a full annulus unsteady computation.

INTRODUCTION

Boundary layer ingestion (BLI) is a disruptive propulsive system architecture considered as one of the main solutions for fuel burn reduction in commercial aircraft. In a BLI configuration the engines are embedded into the airframe, ingesting part of its boundary layer. The aircraft wake is then re-accelerated, reducing the flight power requirement and the thrust specific fuel consumption with respect to an engine in free stream flow (Hardin, et al., 2012) (Hall, 2015) (Atinault, et al., 2013).

Although BLI has been shown to potentially offer up to 10 % gain in fuel burn (Hardin, et al., 2012) (Hall, 2015), applying the BLI concept to an aircraft remains a challenging task. One of the main reasons is the complex aerodynamic interaction that appears between the engine, namely the fan stage, and the airframe. Indeed, the fan aerodynamic effects must be accurately predicted and taken into account in integrated aircraft designs.

As full annulus unsteady RANS computations are unaffordable for daily design loops, reduced-order methodologies have been developed for capturing the fan stage flow physics under inlet distortion. One of the most successful methodologies is body force modeling (Gong, 1999) (Peters, 2014) (Hall, 2015) (Thollet, 2017). This approach consists in replacing the blade rows by a force

Florian Blanc
Airbus Operations

William Thollet
Airbus Operations

field in the Navier-Stokes equations that provides the same flow turning and entropy rise as the actual blades.

While offering accuracy comparable to full annulus unsteady computations in terms of global performance and flow distortion transfer, body force modeling presents a significantly reduced computational cost due to a lower mesh cell count and since a steady approach can be used to conduct non-uniform inflow and outflow computations. However, body force modeling has been found to raise some challenges that might limit its applicability. Firstly, its accuracy relies on predefined model equations that introduce a series of simplifying hypotheses. Secondly, specific blade geometrical features are required for building the model, although they may not be available to an airframe manufacturer.

The goal of the present contribution is to explore a new approach in body force model building. More specifically, it is believed that machine learning techniques are particularly well suited for automatizing the model generation process, and may also attenuate the blade geometry information requirements. For this purpose, the emphasis is put on demonstrating the ability of machine learning techniques in body force modeling.

Firstly, a review of body force modeling and machine learning applications in CFD is presented. Then, the new machine learning approach is described and applied for generating a body force model. Finally, the resulting model is assessed in the prediction of isolated fan performance and distortion transfer in a BLI representative configuration.

BODY FORCE MODEL DEVELOPMENT REVIEW

Body force modeling relies on the idea of representing the blade row aerodynamic effects in the flow by a volume force field generated by redistributing the blade forces in the azimuthal direction. Marble (Marble, 1964) first retrieved the thermodynamic relations that link the flow turning and entropy rise to such forces, and separated both effects into two different force components. Based on this analysis, Gong (Gong, 1999) derived an analytical body force model as a function of the local flow properties and applied it to the prediction of stall inception and inlet distortion response of low speed, multi-stage compressors.

How to cite: Maya Singh and Ethan Kim (2023). Analyzing Fan-Airframe Aerodynamic Interactions using a Machine Learning-Based Body Force Model. Journal of Computer Engineering, 12(6), 51–62. DOI: https://doi.org/10.5281/zenodo.19349209

Later, this model was improved by Peters (Peters, 2014), in order to account for the losses generated in off-design conditions. A calibration process based on reference RANS computations was also introduced and the model was applied to predict short intake – fan aerodynamic interactions. Hall (Hall, 2015) developed an inviscid model that does not require any calibration and used it for computing three-dimensional fan stage response to distortion typical of BLI configurations. A recent improvement in body force modeling is the work of Thollet. Firstly, the metal blockage effects of the turbomachinery blades were taken into account through additional source terms in the equations. The calibration process and loss formulation of Peters were also reviewed, enhancing the model accuracy (Thollet, et al., 2015). Moreover, Hall's model was modified to account for loss generation (Thollet, 2017). Finally, a novel model was derived based on an airfoil lift/drag analogy (Thollet, et al., 2016). These contributions were tested in intake-fan and distorted inflow computations, providing satisfactory results.

Although these analytical models have been successfully applied to the prediction of the complex turbomachinery flows mentioned above, two main drawbacks underlying the model building have been identified. Firstly, the formulations contain a set of adjustable coefficients that must be calibrated using reference computations, thus limiting their accuracy in other conditions. A parallel can be drawn with turbulence model development for the closure of the RANS equations. In this field, the application of machine learning techniques has brought a new perspective for enhancing the accuracy of traditional models. In the previous decade, Milano & Koutmoutsakos (Milano & Koumoutsakos, 2002) proposed to use neural networks for near wall turbulence modeling. More recently, Tracey et al (Tracey, et al., 2015) showed the ability of neural networks to replace an analytical turbulence model. In Tracey's work, a supervised learning algorithm is used to train a neural network to learn the Spalart-Allmaras turbulence model (Spalart & Allmaras, 1994) from reference flows such as a flat plate, a duct or a transonic wing. The neural network is then used to replace the actual turbulence model in a CFD solver, providing accurate results over the set of reference flows. More examples of machine learning-based surrogate modeling of flow physics can be found in the contributions of Zhang & Duraisamy (Zhang & Duraisamy, 2015) (Duraisamy, et al., 2015), who introduced spatial adjustment terms in the $k-\omega$ turbulence model and in the γ transition model, and Ling et al (Ling, et al., 2016), who replaced the linear eddy viscosity model by a machine learned version of the Reynolds stress tensor.

Besides, a second limitation for analytical body force models comes from an aircraft manufacturer point of view. Indeed, the applicability of body force modeling can be limited as the blade geometry is explicitly required to formulate the analytical expressions of the source terms. Unfortunately, this information might not be accessible in an industrial context. It would therefore be desirable to limit the dependency of body force modeling on the blade geometrical description.

The present contribution aims at exploring the applicability of machine learning for building a surrogate body force model, replacing the analytical approach so as to overcome its limitations.

METHODOLOGY

The overall strategy is to build a machine learned body force model from a database of single passage steady computations generated from axisymmetric inflow conditions.

A supervised learning technique is chosen for this purpose. In this approach, the algorithm infers a functional model relating an input $X \in \mathbb{R}^m$ to an output $Y \in \mathbb{R}^n$ from a set of k labelled pairs of observations or training points (X_i, Y_i) with $(1 \leq i \leq k)$.

The mathematical support of the generated model is chosen to be a multi-layer perceptron neural network (Demuth, et al., 2014) because of its ability to approximate any function with only one hidden layer given a sufficient number of neurons (Hornik, et al., 1989) and to make quick predictions in new data once trained. As shown in figure 1, multi-layer perceptron neural networks consist of a series of layers that transform the input $X = [x_1, \ldots, x_m]$ into the output $Y = [y_1, \ldots, y_n]$ by means of basic algebraic operations. The nodes of the layers are composed of neurons that receive a weighted sum of all the elements of the previous layer and perform a basic mathematical operation called activation function. Then the results are fed to the following layer. The training process consists of optimizing the weighting coefficients of the network so as to minimize a loss function that accounts for the prediction error on the training points.

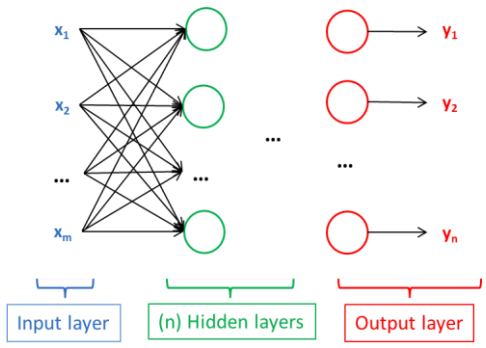

Figure 1: Multi-layer perceptron

The body force model building involves several steps. Firstly, the input and output variables for the supervised learning algorithm are defined. Then, reference CFD computations are conducted and post-processed in order to retrieve the flow field and the body force vector at every

grid location within the blade rows. These quantities are organized in pairs of training instances that constitute the learning database. Model generation is subsequently achieved by training a neural network on the database

$$\frac{\rho f_i h}{\rho e_t} = \mathcal{F}'\left(\frac{V_x}{\sqrt{e_t}}, \frac{V_\theta}{\sqrt{e_t}}, \frac{V_r}{\sqrt{e_t}}, \frac{\Omega r}{\sqrt{e_t}}, x, r\right) \quad (5)$$

As $G = G(x,r)$, the blade geometry effect is captured through the non-dimensional spatial coordinates x and r.

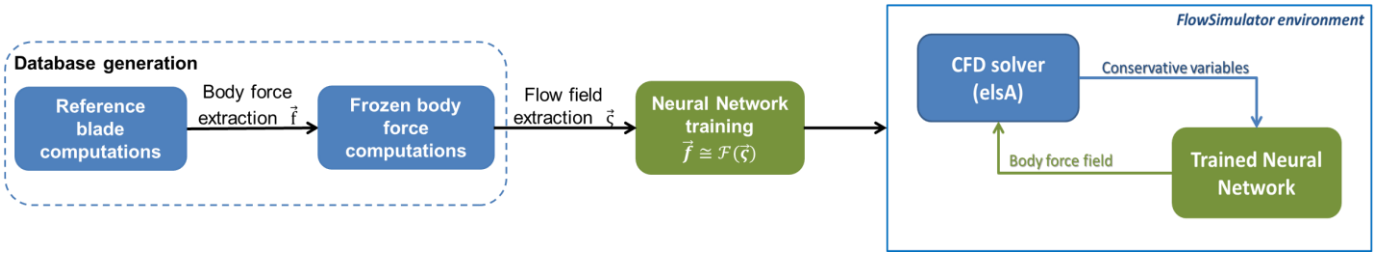

Figure 2: Body force building process

instances. Finally, the models are embedded in a coupling environment for conducting body force computations. This process is depicted in figure 2 and further developed hereafter.

Learning problem formulation

The average flow in a body force-modeled fan stage is described by the RANS equations (viscous flux and heat exchange terms are omitted for clarity):

$$\frac{\partial \rho}{\partial t} + \nabla \cdot \left(\rho \vec{V}\right) = -\frac{1}{b}\left(\rho \vec{V} \cdot \nabla b\right) \quad (1)$$

$$\frac{\partial \rho \vec{V}}{\partial t} + \nabla \cdot \left(\rho \vec{V}\vec{V}\right) = \rho \vec{f} - \nabla P + \frac{1}{b}\left(\rho \vec{V} \cdot \nabla b\right) \cdot \vec{V} \quad (2)$$

$$\frac{\partial \rho e_t}{\partial t} + \nabla \cdot \left(\rho h_t \vec{V}\right) = \rho \Omega f_\theta - \frac{1}{b}\left(\rho \vec{V} h_t \cdot \nabla b\right) \quad (3)$$

Where $\vec{f}$ is the body force vector and b is the metal blockage introduced by the blade thickness, as described in (Thollet, et al., 2015).

Following Gong's analysis (Gong, 1999), the body force is split into two components: a normal component to the relative flow f_n which provides flow turning, and a parallel component f_p accounting for loss generation. Each of them responds to local flow conditions and blade geometric features, and therefore can be expressed as function of the conservative variables, the rotation speed and the blade geometry:

$$\rho f_i = \mathcal{F}(\rho V_x, \rho V_\theta, \rho V_r, \rho e_t, \rho \Omega r, G, h) \quad (4)$$

With $i = n, p$ and $G(x,r)$ being the axisymmetric representation of the local blade geometry. The local bladeto-blade staggered spacing h appears in the equation so as to smear out the blade forces through a blade passage. The main interest in this formulation is that any other flow variable needed to describe the force can be deduced from the previous ones.

It is convenient to reformulate relation (4) into a nondimensional form, hence allowing reducing the dimensionality of the problem. Applying the BuckinghamPi theorem leads to:

Furthermore, the choice of $\sqrt{e_t}$ as a scaling variable is retained since this magnitude remains well-behaved in the entire flow domain, unlike the velocity components in near wall regions for instance. Furthermore, the squared version of the velocity non-dimensional numbers is avoided as ignoring the sign of the velocity components would not allow the machine learning algorithm to retrieve the flow angles.

The goal of the machine learning algorithm is to infer the functional relation $\mathcal{F}$, relating the non-dimensional body force term to the non-dimensional input variables.

Database generation

The flow in fan stages for a BLI-like distorted inflow situation is characterized by a combination of local non-zero absolute swirl angles α, radial flow angles ξ and mass flow rate deficit, resulting from the fan-induced flow redistribution (Hall & Gunn, 2014). Hence, it is proposed to produce two sets of training flow solutions to generate a body force model suitable for a BLI application. The first set consists of a series of operating points along a given speed line with inlet swirl angles of -8°, -5°, -2.5°, 0°, 2.5°, 5° and 8°. The second one corresponds to a series of operating points along the same speed line with a boundary layer-like radial, axisymmetric total pressure profile in which the tip total pressure drops to 80 %, 85% and 90% of the value in the clean flow region.

The first step in the database generation consists of producing the flow solutions for the operating points mentioned above using single passage, mixing plane computations, referred to as "blade" computations. Then, an averaging process is carried out in order to compute the azimuthally averaged flow. Then, the body force components are retrieved using Marble's relations.

In order to obtain a flow solution that is self-consistent with the retrieved force field, the force-flow reconciliation principle of Kerner (Kerner, 2010) is applied. A new set of solutions is generated by imposing the body forces and keeping them invariant with the flow within a fan single passage. Such flow solutions, referred to as "frozen body force" computations, constitute along with the body force

fields the database used to feed the machine learning algorithm. In order to better capture the particularities of the body force physics, the model is subdivided into four parts: a separate sub-model for each force component (f_n and f_p) and for each row in the fan stage (rotor blade and OGV). Each sub-model is contained in a different neural network.

A total of 77 fan operating points were computed for generating the database. Taking into account the mesh resolution, such database contains around 85,000 instances for the rotor row and 60,000 instances for the OGV row. These data sets are then divided in two parts: a training set containing roughly 90 % of the cases and a validation set containing the 10 % remaining. The validation set is used to verify that the neural networks do not suffer from overfitting (Domingos, 2012).

Training

Each sub-model is generated by means of training a multi-layer perceptron neural network of 2 hidden layers, each containing 50 neurons for the rotor models and 40 in the case of the OGV models. The ReLU activation function is chosen for the normal force networks, while the hyperbolic tangent is selected for the parallel force networks. Using standard machine learning best practices, data are pre-processed by means of linearly scaling all inputs and outputs to the same adequate range.

Learning is achieved by performing a mini-batch training (Ruder, 2016) on the parameters of the networks by means of the backpropagation algorithm using a quadratic loss function (Demuth, et al., 2014). The Adam optimizer (Kingma & Ba, 2014) is used for finding the loss function minima. A total of 20,000 epochs were necessary to achieve convergence in all the trainings. The Tensorflow Python library for machine learning applications is used for these purposes (Abadi, et al., 2016).

Computational environment

The machine learned body force models are coupled with the CFD solver elsA (Cambier, et al., 2013) in the FlowSimulator environment (Meinel & Einarsson, 2010) as shown in figure 2. The in-memory coupling proposed by Thollet (Thollet, et al., 2015) is set between the solver and a Python module containing the body force model that exchange information following a fixed-point algorithm. For each grid location, the corresponding neural network is queried to provide the local body force component that is then imposed to the CFD solver to perform a new iteration.

Test case

The assessment of this methodology is done on the NASA/GE R4 fan stage (Hughes, et al., 2002). The characteristics of this fan are summarized below.

Table 1: NASA/GE R4 characteristics

Nb of fan blades	22	Corrected design speed (RPM)	12657
Nb of OGV	54	Stage pressure ratio	1.47
Tip diameter (cm)	0.56	Corrected design mass flow rate (kg/s)	45.6
Hub to tip ratio	0.3	Tip relative Mach number	1.26

Blade computations of the fan are performed using a 3.6 million cell mesh, while the frozen body force mesh contains 110 k cells. An implicit pseudo-time marching method is used to obtain a steady-state solution. Turbulence closure is achieved through the Spalart-Allmaras model. The convective fluxes are treated with a second-order Roe scheme with the Van-Albada limiter. Total conditions are imposed at the computational domain inlet and a throttle condition with radial equilibrium is imposed at the outlet, whose relaxation parameter is modified for computing different operating points along a speed line.

RESULTS AND DISCUSSION

This methodology is assessed at two different fan rotation speeds: the design speed noted as 12657 RPM and a reduced speed of 9809 RPM. A different body force model is generated for each speed line. In a first step, the models are used reproduce the body force field given the CFD flow solution in order to validate the model training. Then, the models are embedded in the computational environment for predicting fan performance under uniform inflow and in a BLI configuration.

Training validation

The trained neural network prediction accuracies are assessed firstly by reproducing the force field corresponding to the training flow solutions and comparing it against the reference CFD force field. The R^2 determination coefficient is used as the metric for this comparison, defined as:

$$R^2 = 1 - \frac{\sum_{i=1}^{N}(f_i^{NN} - f_i^{CFD})^2}{\sum_{i=1}^{N}(f_i^{CFD} - \overline{f^{CFD}})^2} \qquad (6)$$

Where f^{CFD} stands for the body force provided by CFD solution, f^{NN} is the body force predicted by the neural network and N is the number of mesh cells in the body force region.

Table 2 summarizes the determination coefficients for each trained neural network at the considered speeds. As the values from the training set do not differ substantially from those of the validation set, it is concluded that no overfitting occurs (Domingos, 2012).

Model	RPM 9809	RPM 12657
Sub-model	R^2 training	R^2 training
f_n in rotor	0.997	0.993

f_p in rotor	0.991	0.993
f_n in OGV	0.996	0.994
f_p in OGV	0.985	0.954

Table 2: Model determination coefficients

Isolated fan performance

The body force models are first tested for the prediction of the fan performance with axisymmetric inlet flow corresponding to the operating points used for training. For this purpose, machine learned body force computations, referred to as "ML" computations, are conducted for both rotational speeds using the same computational approach as for the frozen body force case. The work coefficient ψ and the total-to-total fan stage efficiency η are compared to

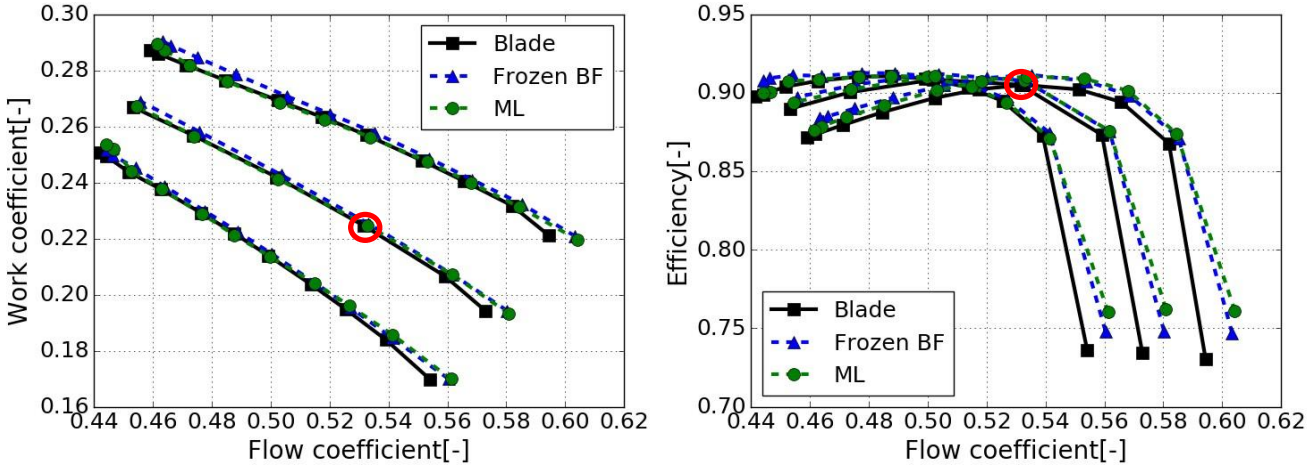

Figure 3: Global performance at 9809 RPM for -5º swirl, no swirl and 5º swirl

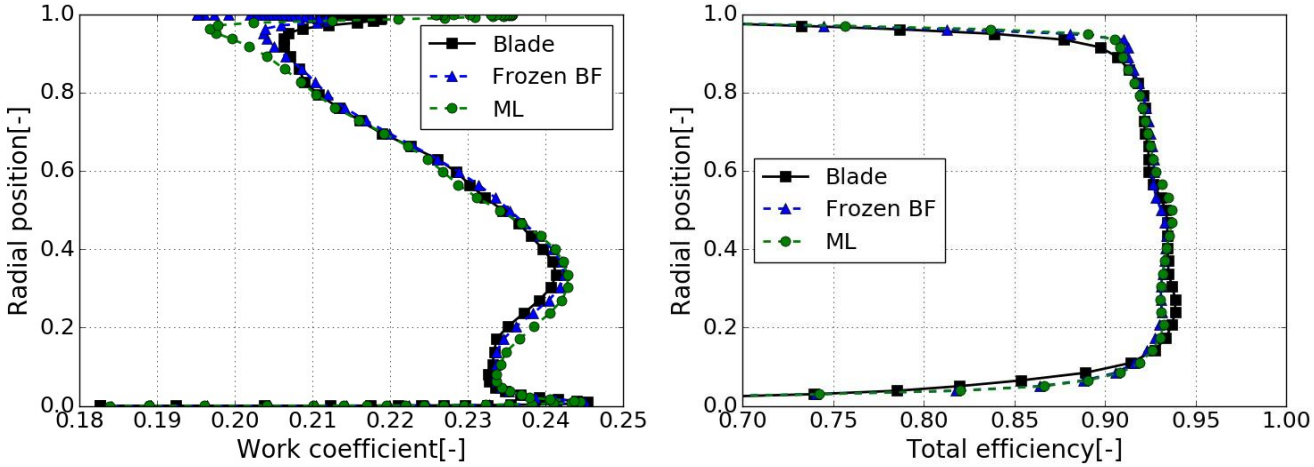

Figure 4: Spanwise performance profiles at peak efficiency for 9809 RPM

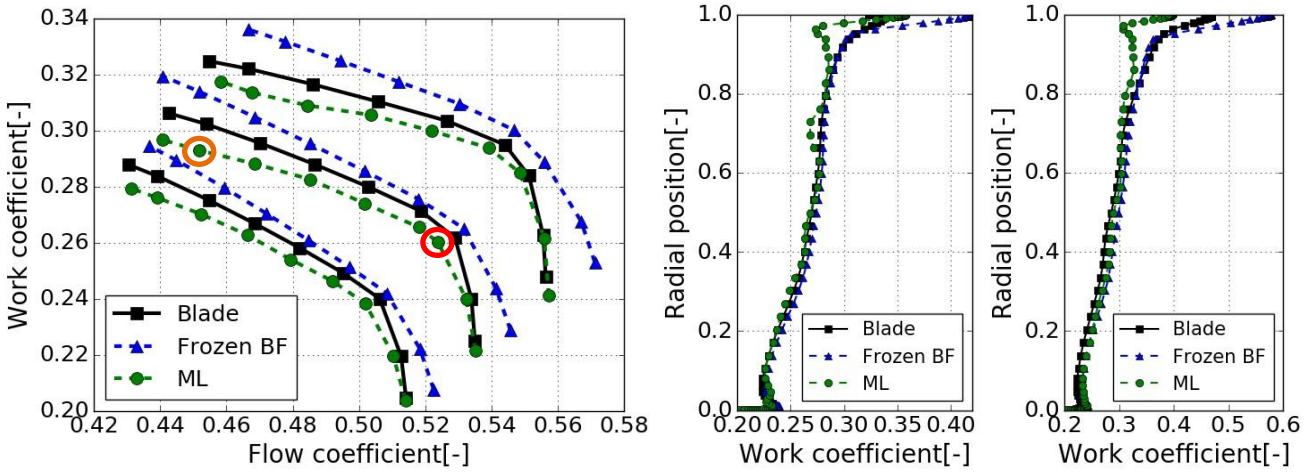

Figure 5: Work coefficient evolution for 12657 RPM for -5º, 0º and 5º swirl (left). Work coefficient spanwise profile with no inlet swirl at the red-marked operating point (center) and at the orange-marked operating point (right)

those obtained in blade computations and frozen body force learned model successfully mimics the frozen body force computations. results, capturing very precisely the evolution of the work coefficient and the efficiency along the speed line with respect to the blade computation.

The global performance of the fan stage is displayed in The spanwise profiles confirm the accuracy of the figure 3 for inlet swirl angles of -5º, 0º and 5º. The machine neural network prediction. Figure 4 shows the work coefficient and efficiency radial distributions at the maximum efficiency operating point with no inlet swirl marked in figure 3. Only minor local differences that do not exceed 5% error can be seen near the tip for the work coefficient between frozen and machine learning body forces.

Performance at 12657 RPM

Some disagreements can be seen for this rotational speed in the fan global performance. As displayed in figure 5, the frozen body force approach leads to substantial differences in the prediction of the choked mass flow rate and the work coefficient in the most loaded operating points. Furthermore, the machine learned model fails to imitate the frozen approach, with differences in the prediction of the global work coefficient that exceed 6 % error near stall without inlet swirl.

The comparison of spanwise profiles evidences the origin of such differences. Figure 5 displays the work coefficient profile at peak efficiency without inlet swirl, showing that frozen body forces over predict the work coefficient near the tip. On the contrary, the machine learned model does not follow this behavior and presents a deficit of work input. These disagreements become more flagrant for a near stall operating point, where local errors of 40% are reached in the tip region.

These results indicate a twofold problem: on the one hand the secondary flows in the tip region hamper a correct retrieval of the body forces from blade computations. On the other hand the neural network fails to reproduce the learned frozen body forces during the computations. In order to address these issues, two actions may be proposed. Firstly, a modified force extraction procedure should be used in the tip region. Secondly, the learning procedure may be enhanced by providing more training instances to the neural networks and eventually adapting their number of neurons.

The BLI case study is carried out at the reduced rotation speed of 9809 RPM. The machine learned body force model generated from single passage computations presented above is directly applied to this three-dimensional case without any modification.

BLI application

The aerodynamic response of the machine learned body force model is assessed hereafter in the presence of a total pressure inlet distortion representative of a BLI configuration. The results are compared against a full annulus URANS computation and the analytical model of Hall modified by Thollet (Thollet, et al., 2016), referred to as the “analytical” body force model. This model consists of a compressible formulation for the normal and parallel force and does not take into account off-design losses in the former one. Hence, the model does not need to be calibrated but might suffer from a lack of accuracy in the off-design efficiency prediction.

A vertically stratified total pressure distortion pattern representative of a boundary layer is imposed at the inlet (figure 6), along with a constant total temperature and a purely axial velocity.

Computations are conducted at the peak efficiency corrected mass flow rate for 9809 RPM. URANS computations are carried out by means of a sliding mesh approach on a 110 million cell mesh, using a second order dual time stepping algorithm. The convective fluxes are treated using a second-order Roe scheme with the Van Albada limiter. Eight revolutions with ten time steps per blade passage followed by one revolution with sixty time steps per passage allow establishing a periodic flow. The computational domain is displayed in figure 7. Three axial stations are considered for comparisons: station 1, for which only instantaneous solutions are available as it lays within the sliding interfaces; and stations 2 and 3, in which the flow is time-averaged in the absolute frame during an additional fan rotation. Total turnaround time was 14 days on 384 cores.

Steady body force computations are conducted with a pseudo-time marching algorithm on a 22 million cell mesh. In the machine learning based body force computations, the Jameson second order centered scheme for convective fluxes is preferred to the Roe upwind scheme, since the former provided a more robust convergence. In all cases the Spalart-Allmaras turbulence model is used. A throttle condition with radial equilibrium is imposed at the outlet and the same

relaxation parameter is kept for all the computations. Body force computations last around 4 hours using 96 cores.

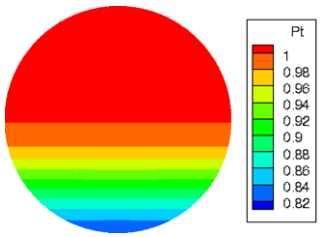

Figure 6: BLI total pressure inlet profile (Hall, 2015)

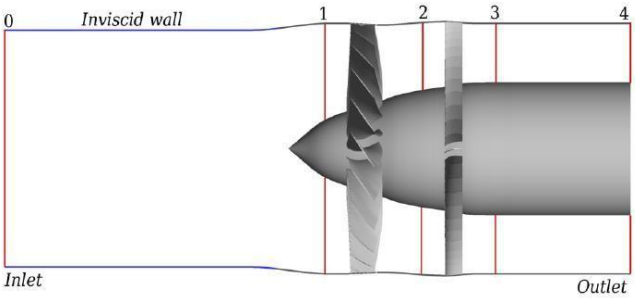

Figure 7: BLI computational domain (Thollet, 2017)

Fan-induced upstream flow redistribution

The fan provides a non-axisymmetric work input in response to the distorted inflow, generating threedimensional flow redistribution upstream of the rotor (Hall & Gunn, 2014). At station 1, the fluid migration from the upper to the lower half-annulus

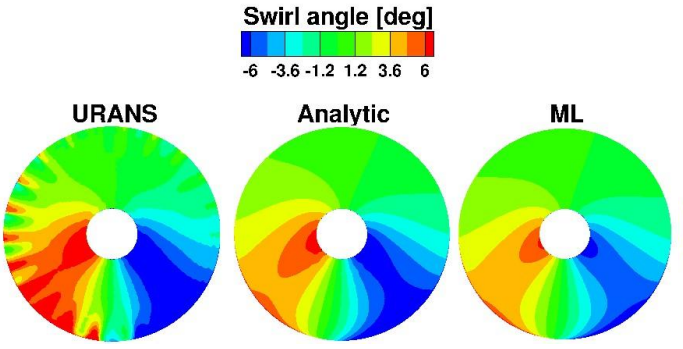

Figure 8: Fan upstream

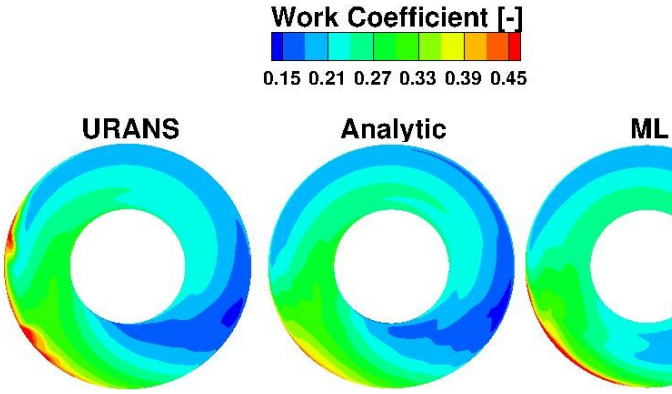

Figure 9: Rotor work

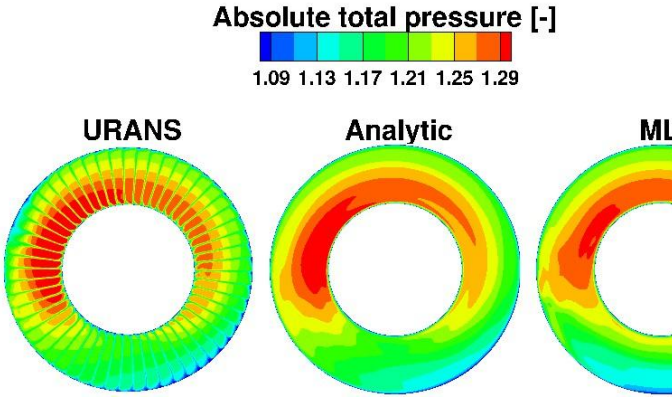

Figure 10: Total pressure dist

generates regions of positive and negative swirl angle. Furthermore, the radial migration from hub to tip in the low-momentum region causes a region

of positive radial angle to appear. Figure 8 shows that the machine learned model successfully captures this fan upstream influence, with only a slight underestimation of the swirl angle peak value region extension as compared to the analytical model and the URANS solution.

Rotor work input

The combination of non-zero absolute swirl angle and axial velocity deficit leads to off-design incidence angles in the whole annulus (Hall & Gunn, 2014). Therefore, the work input of the rotor is not uniform and tends to compensate the stagnation pressure deficit received. Figure 9 shows that the existence of lower and higher work coefficient regions at station 2 is well predicted by the machine learned model; however, the analytical model provides more accurate peak values of these regions as compared to URANS. The azimuthal profiles of this quantity at 25 % and 75% span confirm such an observation.

Distortion transfer through the fan stage

The non-uniform work input and axial velocity downstream of the rotor cause the OGV to operate in offdesign conditions leading to locally increased losses (Hall & Gunn, 2014). As a result of this flow heterogeneity, the total pressure field distortion is transferred throughout the fan stage. Total pressure contours at station 3 reveal an overall agreement between the URANS and the machine learned model prediction, although the azimuthal profiles show some disagreements in the position and peak values of the low total pressure region. Again, the analytical model proves to slightly better reproduce the URANS results. Furthermore, a low pressure region in the upper part of the annulus is captured by the URANS computation evidencing an incipient flow separation. This particularity is not captured by any of the body force models.

Global performance

An adverse effect of the inlet distortion is the reduction of the fan efficiency, which must be accurately predicted to quantify the potential benefits from a BLI configuration. The total to total isentropic efficiency between the domain inlet and station 3 is computed for the machine learned model and compared to the URANS and the analytical model predictions. As displayed in table 3, the machine learned model and the analytical model over predict this efficiency since the incipient near tip separation predicted by the URANS computation is not captured. The machine learned model outperforms the analytical model in this case, due to the simplified loss formulation of the later.

	URANS	Analytic	ML
Work coefficient	0.235	0.231	0.231
Total efficiency	0.873	0.913	0.895

Table 3: Efficiency in BLI computations

CONCLUSIONS

The applicability of machine learning in body force modeling has been investigated. A novel methodology was developed consisting of training a neural network from reference single passage computations, without explicitly using the blade geometry and automatizing the model building. The assessment of the methodology on the isolated fan case showed the ability of the neural network in reproducing the fan performance but also revealed disagreements in highly loaded fan operating points, probably due to the inaccurate body force extraction in the tip region. Although the machine learned models are generated from axisymmetric-inflow single-passage computations, the application to a full-annulus BLI configuration showed the model ability to capture the main three-dimensional flow redistribution mechanisms such as the fan upstream influence, the inhomogeneous rotor work input and total pressure distortion transfer through the fan stage. However, the analytical body force model proved to be slightly more accurate compared to the URANS simulation. Future work will first focus on improving the body force extraction procedure and subsequently on enhancing the accuracy of the machine learned model on BLI applications.

NOMENCLATURE

α	Absolute swirl angle
ξ	Radial flow angle
ρ	Density
V	Absolute flow velocity
b	Metal blockage
f	Body force vector
f_n	Normal body force component
f_p	Parallel body force component
P	Static pressure
e_t	Total energy
Ω	Rotational speed
h_t	Stagnation enthalpy
G	Blade geometry
h	Staggered spacing
$R2$	Determination coefficient
η	Total to total isentropic efficiency

ψ	Work coefficient
OGV	Outlet Guide Vane
ReLU	Rectified Linear Unit

REFERENCES

Abadi, M., Barham, P. & Chen, J., 2016. TensorFlow: A System for Large-Scale Machine Learning. *OSDI,* Volume 16, pp. 265-283.

Atinault, O. et al., 2013. *Numerical and Experimental Aerodynamic Investigations of Boundary Layer Ingestion for Improving Propulsion Efficiency of Future Air Transport*. San Diego, CA, 31st AIAA Applied Aerodynamics Conference.

Cambier, L., Heib, S. & Plot, S., 2013. The Onera elsA CFD software: input from research and feedback from industry. *Mechanics and Industry, EDP science edition,* 14(3), pp. 159-174.

Demuth, H. B., Beale, M. H., De Jess, O. & Hagan, M. T., 2014. *Neural network design*. s.l.:Martin Hagan. Domingos, P., 2012. A few useful things to know about machine learning. *Communications of the ACM,* 55(10), pp. 78-87.

Duraisamy, K., Zhang, Z. J. & Singh, A., 2015. New Approaches in Turbulence and Transition Modeling Using Data-driven Techniques. *AIAA Paper,* Volume 1284.

Gong, Y., 1999. *A Computational Model for Rotating Stall and Inlet Distortions in Multistage Compressors*. s.l.:Doctoral disertation, MIT.

Hall, C. & Gunn, E., 2014. Aerodynamics of boundary layer ingesting fans. *ASME Paper,* Issue GT2014-26142. Hall, D. K., 2015. *Analysis of civil aircraft propulsion with boundary layer ingestion*. s.l.:Doctoral disertation, MIT.

Hardin, L. W., Tillman, G. & Sharma, O. P., 2012. Aircraft System Study of Boundary Layer Ingesting Propulsion. *AIAA paper*.

Hornik, K., Stinchcombe, M. & White, H., 1989. Multilayer feedforwad networks are universal approximators. *Neural Networks,* 2(5), pp. 359-366.

Hughes, H., Jeracki, R., Woodward, W. & Miller, C., 2002. *Fan noise source diagnostic test - rotor alone aerodynamic performance results*. Breckenridge, Colorado, 8th AIAA/CEAS Aeroacoustics Conference and Exhibit. Kerner, J., 2010. *An Assessment of Body Force Representations for Compressor Stall Simulation*. s.l.:Master thesis, MIT.

Kingma, D. & Ba, J., 2014. *Adam: A method for stochastic optimization,* s.l.: arXiv preprint arXiv:1412.6980. Ling, J., Kurzawski, A. & Templeton, J., 2016. Reynolds averaged turbulence modelling using deep neural networks with embedded invariance. *Journal of Fluid Mechanics,* Volume 807, pp. 155-166.

Marble, F., 1964. Three Dimensional Flow in Turbomachines. *High Speed Aerodynamics and Jet Propulsion. Princeton University Press,* Volume X, pp. 83166.

Meinel, M. & Einarsson, G., 2010. *The flowsimulator framework for massively parallel CFD applications*. s.l., PARA 2010 Conference.

Milano, M. & Koumoutsakos, P., 2002. Neural network modeling for near wall turbulent flow. *Journal of Computational Physics,* 182(1), pp. 1-26. Peters, A., 2014. *Ultra-Short Nacelles for Low Fan Pressure Ratio Propulsors*. s.l.:Doctoral disertation, MIT. Ruder, S., 2016. *An overview of gradient descent optimization algorithms,* s.l.: arXiv preprint arXiv:1609.04747.

Spalart, P. & Allmaras, S. R., 1994. A one equation turbulence model for aerodynamic flows. *RECHERCHE AEROSPATIALE-FRENCH EDITION,* Issue 5-5. Thollet, W., 2017. *Body force modeling of fan-airframe interaction*. s.l.:Doctoral disertation, ISAE-Supaero. Thollet, W., Dufour, G., Blanc, F. & Carbonneau, X., 2015. *Body force modeling for aerodynamic analysis of air intakefan intaractions*. Toulouse, 50th 3AF conference on applied aerodynamics.

Thollet, W., Dufour, G., Blanc, F. & Carbonneau, X., 2016. *Assessment of body force methodologies for the analysis of intake-fan aerodynamic interactions*. Seoul, ASME Turbo Expo 2016: Turbomachinery technical conference.

Tracey, B., Duraisamy, K. & Alonso, J. J., 2015. A Machine Learning Strategy to Assist Turbulence Model Development. *AIAA paper,* Issue 1287.

Zhang, Z. J. & Duraisamy, K., 2015. Machine Learning Methods for Data-Driven Turbulence Modeling. *AIAA Aviation,* Volume 2460.